Local Nonreflecting Boundary Condition for Time-Dependent Multiple Scattering

Marcus J. Grote, Imbo Sim

.

Department of Mathematics
University of Basel
Rheinsprung 21
CH - 4051 Basel
Switzerland

Preprint No. 2010-04
Ocotober 10

www.math.unibas.ch

Local Nonreflecting Boundary Condition for Time-Dependent Multiple Scattering[☆]

Marcus J. Grote[*,a], Imbo Sim[b]

[a] *Institute of Mathematics, University of Basel, Rheinsprung 21, 4051 Basel, Switzerland*
[b] *Mathematics Institute of Computational Science and Engineering, EPFL, Station 8, 1015 Lausanne, Switzerland*

Abstract

Starting from a high-order local nonreflecting boundary condition (NBC) for single scattering [25], we derive a local NBC for time-dependent multiple scattering problems, which is completely *local both in space and time*. To do so, we first develop an exterior evaluation formula for a purely outgoing wave field, given its values and those of certain auxiliary functions needed for the local NBC at the artificial boundary. By combining that evaluation formula with the decomposition of the total scattered field into purely outgoing contributions, we obtain a completely local NBC for time-dependent multiple scattering problems. The accuracy and stability of this new local NBC are evaluated by coupling it to a standard finite difference method.

Key words: nonreflecting boundary conditions, absorbing boundary conditions, multiple scattering, time dependent waves, exterior evaluation, far-field evaluation

1. Introduction

Scattering problems in unbounded domains occur in a wide variety of applications such as radar or sonar technology, wireless communications, or seismic imaging. For computation, a well-known approach is to enclose all obstacles, inhomogeneities and nonlinearities with an artificial boundary B.

[☆]This work was supported by the Swiss National Science Foundation.

[*]To whom correspondence should be addressed.

Email addresses: Marcus.Grote@unibas.ch (Marcus J. Grote), Imbo.Sim@epfl.ch (Imbo Sim)

A boundary condition is then imposed on B, which leads to a numerically solvable boundary value problem in the finite computational domain Ω. The boundary condition should be chosen such that the solution of the problem in Ω coincides with the restriction to Ω of the solution in the original unbounded region. Otherwise it will induce spurious reflections at B, which will travel back into Ω and distort the numerical solution everywhere.

When Ω is convex, all waves leaving the computational domain are purely outgoing and never return. Many approaches are then available to effectively truncate the infinite exterior, such as the popular perfectly matched layer (PML) approach [7, 8, 10, 22], but also nonlocal nonreflecting boundary conditions (NBC) [17, 18, 30], or infinite elements [4] – see [33, 24] for a review. In particular, Hagstrom and Hariharan [25] derived a new formulation of the classical Bayliss and Turkel [6] conditions of arbitrarily high order, yet without high order derivatives. It holds for B a sphere and is local both in space and time, while its high accuracy and efficiency in computations was shown in [28]. Similarly, Givoli and Neta [15] and Hagstrom and Warburton [26] each proposed a reformulation of the Higdon [27] conditions without high order derivatives for rectangular B – see [14] for a recent review.

However, when the scatterer consists of several obstacles which are well separated from each other, the use of a single artificial boundary to enclose the entire (convex) scattering region becomes too expensive. Instead it is preferable to enclose every sub-scatterer by a separate artificial boundary B_j. Then we seek an exact boundary condition on $B = \bigcup B_j$, where each B_j surrounds a single computational sub-domain Ω_j. Then $\Omega = \bigcup \Omega_j$ is no longer convex and any NBC at B must not only let outgoing waves leave Ω_j without spurious reflection from B_j, but also propagate the outgoing wave from Ω_j to all other sub-domains, which it may reenter subsequently. Hence to derive an exact nonreflecting boundary condition for such *multiple scattering* problems, an analytic representation of the solution everywhere in the exterior region is needed to propagate the outgoing waves to the other sub-domains. Perfectly matched layers, in particular, do not provide such an expression and thus cannot be used.

Boundary conditions based on boundary integral equations [32, 23, 31] can be used regardless of the shape of Ω, and hence also in situations of multiple scattering. The update of the solution at any particular point on the artificial boundary then requires a space-time integral over past values on B. Thus, they are nonlocal both in space and time, while any straightforward implementation will result in a boundary condition one order of magnitude

more expensive than the numerical method used inside Ω. Much current research in integral equation based formulations is devoted to reducing that computational cost [9, 12, 5]. Alternatively, Grote and Kirsch [21] recently derived a NBC for time dependent multiple scattering problems, which is local in time but nonlocal over B. It is the time dependent counterpart of the Dirichlet-to-Neumann condition for exterior Helmholtz problems [19, 13], which was extended to time-harmonic multiple scattering problems in [20] and used for scattering from multiple complexly shaped obstacles in [1].

In this work we shall show how to derive a NBC for time-dependent multiple scattering problems, which is completely *local both in space and time*. Following [21], we first recall in Section 2 how to decompose the scattered field into multiple purely outgoing waves. The scattered field at any particular boundary B_j then consists of an outgoing part and an incoming part, where the latter is determined by its past values on the other boundaries. The use of this decomposition to derive an exact NBC is first illustrated in the simple situation of multiple scattering in one space dimension, where exterior evaluation simply consists in information transfer along characteristics. Next in Section 3, we derive an exterior evaluation formula for an outgoing time dependent three-dimensional wave field, when the high-order NBC by Hagstrom and Hariharan [25] for single scattering is used at B. By combining that exterior evaluation formula with the decomposition from Section 2 and the high-order NBC, we thus obtain a local NBC for time-dependent multiple scattering problems in three space dimensions. In Section 4, we show how to couple it with a standard finite difference scheme and efficiently evaluate the exterior field on B. Finally, in Section 5, we demonstrate the accuracy and usefulness of our local NBC through numerical experiments.

2. Nonreflecting boundary conditions for multiple scattering

2.1. General formulation

We consider acoustic wave scattering from two bounded disjoint scatterers in unbounded three-dimensional space. Each scatterer may contain one or several obstacles, inhomogeneities, and nonlinearity. We let Γ denote the piecewise smooth boundary of all obstacles and impose on Γ a Dirichlet-type boundary condition, for simplicity. In Ω_∞, the unbounded region outside Γ,

the scattered field u then solves the following initial-boundary value problem:

$$\frac{\partial^2 u}{\partial t^2} - \nabla \cdot \left(c^2 \nabla u\right) = f \qquad \text{in } \Omega_\infty, \quad t > 0, \tag{1}$$

$$u = u_0, \quad \frac{\partial u}{\partial t} = v_0 \qquad \text{in } \Omega_\infty, \quad t = 0, \tag{2}$$

$$u = g \qquad \text{on } \Gamma, \quad t > 0. \tag{3}$$

The wave speed $c > 0$ may vary in space, while both f and g may vary in space and time; f may also be nonlinear.

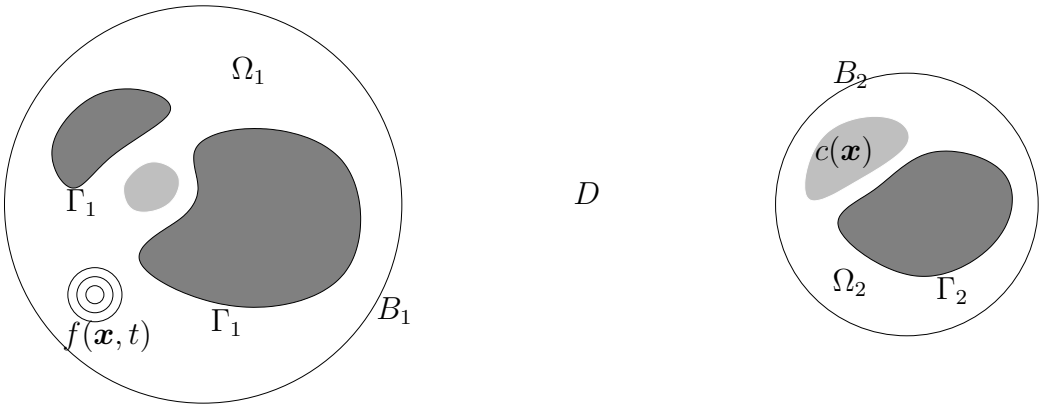

Figure 1: A typical configuration with two scatterers is shown. Each scatterer consists of possibly several obstacles bounded by Γ_1 and Γ_2, but may also contain inhomogeneity, anisotropy, nonlinearity and sources. The computational domain $\Omega = \Omega_1 \cup \Omega_2$ is externally bounded by the artificial boundary $B = B_1 \cup B_2$; the unbounded region outside Ω is denoted by D.

Next, we assume that both scatterers are *well separated,* that is we assume that we can surround them by two non-intersecting spheres B_1, B_2 with radii R_1, R_2, respectively. In the unbounded region, D, outside the two spheres, we assume that the medium is homogeneous and isotropic; moreover, we assume that the source f and the initial values u_0, v_0 vanish in D. In the exterior region, the scattered wave u therefore satisfies the homogeneous wave equation with constant wave speed c and homogeneous initial conditions,

$$\frac{\partial^2 u}{\partial t^2} - c^2 \Delta u = 0 \quad \text{in } D, \quad t > 0, \tag{4}$$

$$u = 0, \qquad \frac{\partial u}{\partial t} = 0 \quad \text{in } D, \quad t = 0. \tag{5}$$

Hence in D, the wave field u is entirely driven by its boundary values at B and purely radiating at large distance.

We wish to compute the scattered field, u, in the computational domain $\Omega = \Omega_\infty \setminus D$, which consists of the two disjoint components Ω_1 and Ω_2. Hence Ω is internally bounded by $\Gamma = \Gamma_1 \cup \Gamma_2$, and externally by $B = \partial D$, which consists of the two spheres B_1 and B_2 – see Fig. 1. To solve the scattering problem (1)–(3) inside Ω, a boundary condition is needed at the exterior *artificial boundary* $B = B_1 \cup B_2$. This boundary condition must ensure that the solution in Ω, with that boundary condition imposed on B, coincides with the restriction to Ω of the solution in the original unbounded region Ω_∞.

In contrast to a situation of single scattering [25, 30, 17], we cannot simply expand u outside B either in Fourier series or as a superposition of purely outgoing radial multipole fields. Indeed, since part of the scattered field leaving Ω_1 will reenter Ω_2 at later times, and vice versa, u is not outgoing in D. Hence, the boundary condition we seek at B must not only let outgoing waves leave Ω_1, say, without spurious reflection from B_1, but also propagate those waves to Ω_2, and so forth, without introducing any spurious reflection.

Now let D_1 denote the unbounded region outside B_1 and D_2 the unbounded region outside B_2. Then the total scattered field u admits the unique decomposition

$$u = u_1 + u_2 \quad \text{in } D = D_1 \cap D_2, \quad t \geq 0, \tag{6}$$

where u_1 and u_2 solve the following two homogeneous wave equations [21]:

$$\frac{\partial^2 u_1}{\partial t^2} - c^2 \Delta u_1 = 0 \qquad \text{in } D_1, \quad t > 0, \tag{7}$$

$$u_1 = 0, \qquad \frac{\partial u_1}{\partial t} = 0 \qquad \text{in } D_1, \quad t = 0, \tag{8}$$

and

$$\frac{\partial^2 u_2}{\partial t^2} - c^2 \Delta u_2 = 0 \qquad \text{in } D_2, \quad t > 0, \tag{9}$$

$$u_2 = 0, \qquad \frac{\partial u_2}{\partial t} = 0 \qquad \text{in } D_2, \quad t = 0. \tag{10}$$

Since u_1 and $\partial_t u_1$ vanish at $t = 0$, u_1 is a purely outgoing wave as seen from B_1, propagating with finite speed c into D_1, and similarly for u_2. Note that u_1 and u_2 are entirely determined by their values on B_1 and B_2, respectively.

The above decomposition (6) of the scattered field u into purely outgoing wave fields is crucial for the derivation of a NBC in a situation of multiple scattering. Indeed when applying a differential operator to u at B, we can thus distinguish the two separate contributions from the incoming and outgoing wave fields, which need to be treated differently. At B_1, for instance, we shall determine the outgoing contribution by applying a local NBC for single scattering [25] to u_1. In contrast, the contribution from u_2 will be determined from its past values at B_2 through an exterior evaluation formula. Before we proceed in Section 3 with the derivation of the NBC in the general three-dimensional setting, we shall illustrate the basic principle underlying the derivation of a NBC for multiple scattering problems in the much simpler one-dimensional case.

2.2. One-dimensional multiple scattering

Here we consider the following one-dimensional Cauchy problem:

$$\begin{aligned} &\frac{\partial^2 u}{\partial t^2} - \frac{\partial^2 u}{\partial x^2} = f(x,t), \qquad -\infty < x < \infty, \quad t > 0, \\ &u(x,0) = u_0(x), \qquad u_t(x,0) = v_0(x). \end{aligned} \tag{11}$$

We assume that the initial disturbance and the forcing are supported inside the region $\Omega = \Omega_1 \cap \Omega_2$, with $\Omega_1 = [0,\, B_1]$ and $\Omega_2 = [B_2,\, L]$, $\quad 0 < B_1 < B_2 < L$, that is $\mathrm{supp}\{u_0,\, v_0,\, f(\cdot,t)\} \subset \Omega$, as illustrated in Fig. 2. We now wish to restrict the computation to the sub-region Ω; therefore we need to impose appropriate boundary conditions at $x = 0$, B_1, B_2, and L to ensure that the solution in Ω coincides with the solution u of the original Cauchy problem for all time.

Since u is purely outgoing for $x < 0$ and $x > L$, the exact NBC at $x = 0$ or $x = L$ corresponds to the standard absorbing boundary condition for single scattering, that is

$$\begin{aligned} &\left(\frac{\partial}{\partial x} - \frac{\partial}{\partial t}\right) u = 0, \quad x = 0, \\ &\left(\frac{\partial}{\partial x} + \frac{\partial}{\partial t}\right) u = 0, \quad x = L. \end{aligned} \tag{12}$$

We now focus on the two remaining artificial boundary points at $x = B_1$ and $x = B_2$, where u is not purely outgoing. Since u satisfies the homogeneous wave equation in $[B_1,\, B_2]$, it is the superposition of a left and right

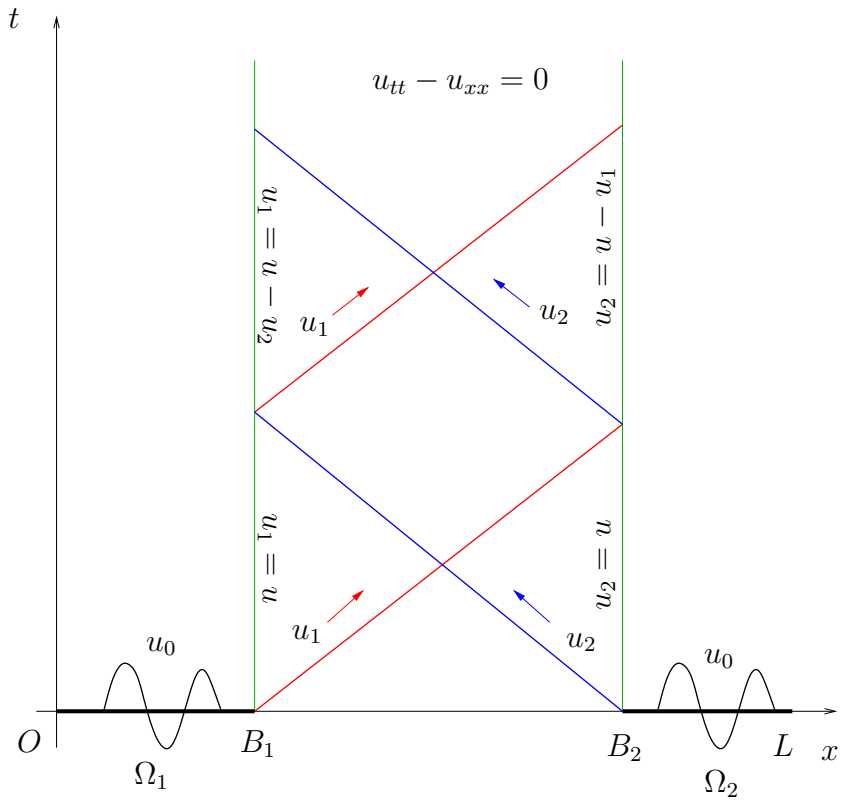

Figure 2: Multiple scattering in one space dimension. The computational domain Ω consists of the two disjoint intervals $\Omega_1 \bigcup \Omega_2$.

moving wave there, that is

$$u(x,t) = u_1(x,t) + u_2(x,t), \tag{13}$$

with

$$u_1(x,t) = f(x-t), \qquad u_2(x,t) = g(x+t). \tag{14}$$

Moreover, if we require that $\text{supp}\{u_1\} \subset \Omega_1$ and $\text{supp}\{u_2\} \subset \Omega_2$ at $t = 0$, u_1 and u_2 are uniquely defined for all time [21]. From (13) and (14) we thus immediately find the exact NBC at $x = B_1$,

$$\begin{aligned} \left(\frac{\partial}{\partial x} + \frac{\partial}{\partial t}\right) u &= \left(\frac{\partial}{\partial x} + \frac{\partial}{\partial t}\right) u_1 + \left(\frac{\partial}{\partial x} + \frac{\partial}{\partial t}\right) u_2 \\ &= \left(\frac{\partial}{\partial x} + \frac{\partial}{\partial t}\right) u_2, \end{aligned} \tag{15}$$

since u_1 is outgoing here.
Thus to impose the exact NBC at $x = B_1$, we must be able to evaluate u_2 there. In doing so, we need to distinguish initial times up to $t = B_2 - B_1$ from later times $t \geq B_2 - B_1$:

- $0 \leq t < B_2 - B_1$: due to the finite propagation speed (here set to one), u_2 hat not reached Ω_1 yet; hence, u_2 is still zero at $x = B_1$ and (15) reduces to the standard NBC for purely outgoing solutions.
- $B_2 - B_1 \leq t$: u_2 no longer vanishes at $x = B_1$; however, u_2 is fully determined by its past values at $x = B_2$ as

$$u_2(B_1, t) = u_2(B_2, t - (B_2 - B_1)). \tag{16}$$

Yet how do we determine u_2 at $x = B_2$? Recall that we are only computing u inside Ω. Again during initial times $t < B_2 - B_1$, we have $u_2 = u$ at $x = B_2$. At later times, we determine u_2 at $x = B_2$ from (13) by subtracting from u the value of u_1 there, which itself is now determined through (14) by its past values on B_1, that is

$$\begin{aligned} u_2(B_2, t) &= u(B_2, t) - u_1(B_2, t) \\ &= u(B_2, t) - u_1(B_1, t - (B_2 - B_1)). \end{aligned} \tag{17}$$

Hence at every time step of the numerical scheme, we concurrently update the new values of u_1 and u_2 at $x = B_1$, B_2, respectively. This requires the additional storage of past values of u_i at $x = B_i$, $i = 1, 2$, for the finite time window $[t - (B_2 - B_1), t]$, which corresponds to the travel time between Ω_1 and Ω_2. By keeping track of u and u_i at B_i during that finite time window, we can evaluate them at B_i for all time.

3. Local NBC in three space dimensions

The derivation of a NBC for multiple scattering problems requires three main ingredients: a decomposition of the scattered field into purely outgoing wave fields, a NBC for outgoing waves, and an exterior evaluation formula. Starting from a high-order NBC for single scattering, we shall derive an exterior evaluation formula for the scattered field, which uses only past values of the solution and certain auxiliary functions at B needed for the boundary condition. Similarly to the one-dimensional case described in the previous section, we finally obtain a NBC for time-dependent multiple scattering problems in three space dimensions.

3.1. Local NBC for single scattering

Let B be the sphere of radius R and assume that u satisfies the homogeneous wave equation,

$$\frac{\partial^2 u}{\partial t^2} - c^2 \Delta u = 0, \qquad r > R, \quad t > 0 \tag{18}$$

with zero initial condition outside B,

$$u = 0, \qquad \frac{\partial u}{\partial t} = 0, \qquad r > R, \quad t = 0. \tag{19}$$

Starting from the convergent series [34]

$$u(r, \theta, \phi, t) = \sum_{j=1}^{\infty} \frac{f_j(ct - r, \theta, \phi)}{r^j}, \qquad r > R, \tag{20}$$

where r, θ, ϕ are spherical coordinates, Hagstrom and Hariharan [25] derived the following exact local NBC in three space dimensions:

$$\begin{aligned} \Big(\frac{1}{c}\frac{\partial}{\partial t} + \frac{\partial}{\partial r} + \frac{1}{r}\Big) u &= w_1, \\ \Big(\frac{1}{c}\frac{\partial}{\partial t} + \frac{k}{r}\Big) w_k &= \frac{1}{4R^2}\Big(k(k-1) + \Delta_S\Big) w_{k-1} + w_{k+1} \end{aligned} \tag{21}$$

for $k = 1, 2, \ldots$, and $w_0 = 2u$. Here, Δ_S denotes the Laplace-Beltrami operator in spherical coordinates (r, θ, ϕ),

$$\Delta_S = \frac{1}{\sin\theta}\frac{\partial}{\partial\theta}\Big(\sin\theta \frac{\partial}{\partial\theta}\Big) + \frac{1}{\sin^2\theta}\frac{\partial^2}{\partial\phi^2}. \tag{22}$$

In fact Bayliss and Turkel [6] used the same infinite series representation to derive their hierarchy of local absorbing boundary conditions in spherical coordinates. Similar to the boundary conditions of Engquist and Majda [11], it also requires increasingly higher order derivatives for improved accuracy.

In contrast, the boundary condition (21) is local in space and time and does not involve high-order derivatives, but instead an infinite sequence of auxiliary variables w_k defined on B. In practice, only a finite number of auxiliary functions w_k, $k = 1, \ldots, P$ is used setting $w_{P+1} = 0$. Then, in general the boundary condition is no longer exact, but it *remains exact* for solutions which consist of a *finite* combination of spherical harmonics up

to order P. Imposition of the boundary condition at any fixed radius R thus yields at least spectral accuracy for smooth wave fields with increasing P. Therefore (21) is exact in the same sense as the NBC proposed in [17, 18], namely that P can always be chosen sufficiently large so that the error introduced at B is smaller than the discretization error inside Ω, without moving B farther away from the scatterer. However, this new boundary condition does not require any spherical harmonics or inner products with them; hence, it is somewhat easier and cheaper to implement. The usefulness and accuracy of the NBC (21) was illustrated via numerical experiments in [28]. It was also recently extended to Maxwell's equations in three space dimensions [16].

3.2. Exterior evaluation

Given the values of u and the auxiliary functions $w_1, \ldots, w_P$ in (21) at B, the sphere of radius R, we shall now derive an explicit formula to evaluate u everywhere in the exterior of B. For $r \geq R$, the general solution to (18) is given by the Fourier series representation,

$$u(r, \theta, \phi, t) = \sum_{n=0}^{\infty} \sum_{m=-n}^{n} u_{nm}(r, t)\, Y_{nm}(\theta, \phi), \tag{23}$$

where the spherical harmonics Y_{nm} are defined by

$$Y_{nm}(\theta, \phi) = \sqrt{\frac{2n+1}{4\pi} \frac{(n-|m|)!}{(n+|m|)!}} P_n^{|m|}(\cos\theta) e^{im\phi} \tag{24}$$

and the Fourier coefficients u_{nm} satisfy

$$u_{nm}(r, t) = \sum_{k=0}^{\infty} r^{-k-1}\ f_{nm}^k(ct - r). \tag{25}$$

The spherical harmonics Y_{nm} form a complete L^2-orthogonal system on B. Moreover, they are eigenfunctions of the Laplace-Beltrami operator:

$$\Delta_S\, Y_{nm} = -n(n+1)\, Y_{nm}. \tag{26}$$

By introducing the series representation (23), (25) into (18), we obtain the recursion

$$\left(f_{nm}^{k+1}\right)' = -\frac{k(k+1) - n(n+1)}{2(k+1)} f_{nm}^k. \tag{27}$$

Hence for $k > n$, we may choose $f_{nm}^k = 0$ so that

$$\begin{aligned} u_{nm}(r,t) &= \sum_{k=0}^{n} r^{-k-1}\ f_{nm}^k(ct-r) \\ &= r^{-1}\ f_{nm}^0(ct-r) + \sum_{k=1}^{n} r^{-k-1}\ f_{nm}^k(ct-r). \end{aligned} \tag{28}$$

Next, we multiply (28) by r to obtain at $r = R$:

$$f_{nm}^0(ct-R) = Ru_{nm}(R,t) - \sum_{k=1}^{n} R^{-k} f_{nm}^k(ct-R). \tag{29}$$

By using (29) at time $t-(r-R)/c$ instead of t, we can rewrite (28) as

$$\begin{aligned} u_{nm}(r,t) &= r^{-1}\ f_{nm}^0\big(c(t-(r-R)/c)-R\big) + \sum_{k=1}^{n} r^{-k-1}\ f_{nm}^k(ct-r) \\ &= r^{-1}Ru_{nm}(R,t-(r-R)/c) - r^{-1}\sum_{k=1}^{n} R^{-k}\ f_{nm}^k(ct-r) \\ &\quad + \sum_{k=1}^{n} r^{-k-1}\ f_{nm}^k(ct-r). \end{aligned} \tag{30}$$

We now assume that the solution u consists of a finite number of spherical harmonics up to order P and use (30) to replace u_{nm} in (23). This yields

$$\begin{aligned} u(r,\theta,\phi,t) = Rr^{-1} &\sum_{n=0}^{P}\sum_{m=-n}^{n} u_{nm}(R,t-(r-R)/c)\ Y_{nm} \\ + r^{-1} &\sum_{n=1}^{P}\sum_{m=-n}^{n}\sum_{k=1}^{n}\big(r^{-k}-R^{-k}\big)\ f_{nm}^k(ct-r)\ Y_{nm}. \end{aligned} \tag{31}$$

By using the identity

$$\sum_{n=1}^{P}\sum_{k=1}^{n} a_{n,k} \;=\; \sum_{\ell=0}^{P-1}\sum_{n=p-\ell}^{P} a_{n,P-\ell} \tag{32}$$

with $a_{n,k} = \sum_{m=-n}^{n}(r^{-k}-R^{-k})\ f_{nm}^k(ct-r)\ Y_{nm}(\theta,\phi)$, we rewrite the last term on the right of (31). Then we evaluate the resulting expression at the

future time $t + (r - R)/c$ and recall that $w_0 = 2u$. This yields the following exterior evaluation formula at $r > R$:

$$\begin{aligned} u(r, \theta, \phi, t + (r - R)/c) =& \frac{R}{2r} w_0(R, \theta, \phi, t) \\ &+ \frac{1}{r} \sum_{\ell=0}^{P-1} (r^{\ell - P} - R^{\ell - P})\, \eta_{P,\ell}(R, \theta, \phi, t), \end{aligned} \tag{33}$$

where $\eta_{P,\ell}$ is defined as

$$\eta_{P,\ell}(r, \theta, \phi, t) = \sum_{n=P-\ell}^{P} \sum_{m=-n}^{n} f_{nm}^{P-\ell}(ct - r)\, Y_{nm}(\theta, \phi). \tag{34}$$

We emphasize that we do not need the (unknown) functions $\eta_{P,\ell}$ to evaluate the solution outside B. Instead, we shall now express them in terms of the auxiliary functions w_j to obtain a useful evaluation formula for u.

First, we recall from [[25], p. 408, equations (38), (39)] that

$$w_j(r, \theta, \phi, t) = \sum_{n=j}^{P} \sum_{k=j}^{n} \gamma_{k,j} r^{-k-j-1} \sum_{m=-n}^{n} f_{nm}^{k}(ct - r) Y_{nm}(\theta, \phi), \tag{35}$$

where

$$\gamma_{k,j} = (-1)^j 2^{1-j} \frac{k!}{(k-j)!}. \tag{36}$$

For fixed j, we now let $s = P - k$ and use that $f_{n,m}^{P-s} = 0$ for $s < P - n$ to obtain

$$w_j = \sum_{s=0}^{P-j} \gamma_{P-s,j}\; r^{-P+s-j-1} \sum_{n=j}^{P} \sum_{m=-n}^{n} f_{nm}^{P-s}\; Y_{nm}. \tag{37}$$

Again since $f_{n,m}^{P-s} = 0$ for $n < P - s$, we can rewrite (37) as

$$w_j = \sum_{s=0}^{P-j} \gamma_{P-s,j}\; r^{-P+s-j-1} \sum_{n=P-s}^{P} \sum_{m=-n}^{n} f_{nm}^{P-s}\; Y_{nm} \tag{38}$$

and then use (34) to obtain

$$w_j = \sum_{s=0}^{P-j} \gamma_{P-s,j}\; r^{-P+s-j-1}\; \eta_{P,s}. \tag{39}$$

Next, we separate the term $s = P - j$ from the sum to rewrite (39) as

$$w_j = \gamma_{j,j}\, r^{-2j-1}\, \eta_{P,P-j} + \sum_{s=0}^{P-j-1} \gamma_{P-s,j}\, r^{-P+s-j-1}\, \eta_{P,s}. \tag{40}$$

We now let $k = P - j$ and solve (40) for $\eta_{P,k}$, which yields

$$\begin{aligned} \eta_{P,k} &= (\gamma_{P-k,P-k})^{-1}\ r^{2(P-k)+1}\, w_{P-k} - \sum_{s=0}^{k-1} (\gamma_{P-k,P-k})^{-1}\, \gamma_{P-s,P-k}\, r^{s-k}\, \eta_{P,s} \\ &= \alpha_{P-k}\, r^{2(P-k)+1}\, w_{P-k} - \sum_{s=0}^{k-1} \binom{P-s}{k-s} r^{s-k}\, \eta_{P,s}\ , \end{aligned} \tag{41}$$

where α_j is defined as

$$\alpha_j = (-1)^j 2^{j-1}/j!\ . \tag{42}$$

Next, we evaluate (41) at $r = R$ and rewrite it as

$$\sum_{s=0}^{k} \binom{P-s}{k-s} R^{s-k}\, \eta_{P,s} = \alpha_{P-k}\, R^{2(P-k)+1}\, w_{P-k}, \qquad k = 0, 1, \ldots, P. \tag{43}$$

By multiplying (43) by R^k and defining

$$\tilde{\eta}_s = R^s \eta_{P,s}, \qquad b_k = \alpha_{P-k}\, R^{2P-k+1}\, w_{P-k}, \tag{44}$$

we can rewrite the resulting equation as

$$\sum_{s=0}^{k} \binom{P-s}{k-s} \tilde{\eta}_s = b_k, \qquad k = 0, 1, \ldots, P. \tag{45}$$

Equation (45) is a $(P+1) \times (P+1)$ lower triangular system for $\tilde{\eta}_s$, $s = 0, \ldots, P$. Its solution is

$$\tilde{\eta}_k = \sum_{j=0}^{k} (-1)^{k-j} \binom{P-j}{k-j} b_j, \tag{46}$$

as shown in the Appendix.

In (46) we now replace $\tilde{\eta}_k$ and b_j by their definitions in (44) and the index j by $k-j$, which leads to the following expression for $\eta_{P,k}$ in terms of the auxiliary functions w_k:

$$\eta_{P,k} = \sum_{j=0}^{k} (-1)^j \binom{P-k+j}{j} \alpha_{P-k+j}\, R^{2(P-k)+j+1} w_{P-k+j}. \tag{47}$$

To derive an exterior evaluation for u in terms of the auxiliary functions w_k only, we now use (47) to replace $\eta_{P,\ell}$ in (33). If we denote by $\hat{t} = t - (r-R)/c$ the time retarded value that corresponds to the travel time from R to r, $r > R$, we thus obtain

$$\begin{aligned} u(r,\theta,\phi,t\,) &= \frac{R}{2r}\, w_0(R,\theta,\phi,\hat{t}\,) \\ + \quad & r^{-1} \sum_{k=0}^{P-1} \sum_{j=0}^{k} (-1)^j \binom{P-k+j}{j} \alpha_{P-k+j}\, w_{P-k+j}\left(R,\theta,\phi,\hat{t}\,\right) \left(r^{k-P} R^{2(P-k)+j+1} - R^{P-k+j+1}\right). \end{aligned}$$

We now reorder the double sum above according to the identity

$$\sum_{k=0}^{P-1} \sum_{j=0}^{k} a_{k,j} = \sum_{k=0}^{P-1} \sum_{j=0}^{P-k-1} a_{k+j,j}\ , \tag{48}$$

which yields

$$\begin{aligned} u(r,\theta,\phi,t\,) &= \frac{R}{2r}\, w_0(R,\theta,\phi,\hat{t}\,) \\ + \ & \frac{R}{r} \sum_{k=0}^{P-1} \alpha_{P-k} w_{P-k}(R,\theta,\phi,\hat{t}\,) R^{P-k} \sum_{j=0}^{P-k-1} (-1)^j \binom{P-k}{j} \left(\left(\frac{R}{r}\right)^{P-k-j} - 1 \right). \end{aligned} \tag{49}$$

Next, we use the identity

$$\sum_{j=0}^{\ell-1} (-1)^j \binom{\ell}{j} = (-1)^{\ell-1} \tag{50}$$

with $\ell = P-k$ to rewrite (49) as

$$\begin{aligned} u(r,\theta,\phi,t) &= \frac{R}{2r}\, w_0(R,\theta,\phi,\hat{t}\,) \\ + \quad & \frac{R}{r} \sum_{k=0}^{P-1} \alpha_{P-k} w_{P-k}(R,\theta,\phi,\hat{t}\,) R^{P-k} \left[\sum_{j=0}^{P-k-1} \binom{P-k}{j} \left(\frac{R}{r}\right)^{P-k-j} (-1)^j - (-1)^{P-k-1} \right]. \end{aligned} \tag{51}$$

In (51), the last term inside the square brackets simply corresponds to the term in the sum with $j = P - k$. Moreover, from the binomial formula we have that

$$\sum_{j=0}^{P-k} \binom{P-k}{j} \left(\frac{R}{r}\right)^{P-k-j} (-1)^j = \left(\frac{R}{r} - 1\right)^{P-k}. \tag{52}$$

Hence, the square bracketed term in (51) simplifies to the expression on the right of (52). After replacing α_{P-k} by its definition in (42) and further simplifications, we obtain the exterior evaluation formula:

$$u(r,\theta,\phi,t) = \frac{R}{r} \sum_{k=0}^{P} \frac{2^{k-1}}{k!} \left(R\left(1 - \frac{R}{r}\right)\right)^k w_k(R,\theta,\phi,\hat{t}). \tag{53}$$

We summarize this result as a theorem.

Theorem 1. *Let $u(r,\theta,\phi,t)$ be a solution of (18), (19) that consists of a finite number of spherical harmonics Y_{nm} up to order $n \leq P$ and the auxiliary functions w_j, $0 \leq j \leq P$, satisfy (21) at $r = R$. Then for $r > R$, u satisfies*

$$u(r,\theta,\phi,t) = \frac{R}{r} \sum_{k=0}^{P} \frac{2^{k-1}}{k!} \left(R\left(1 - \frac{R}{r}\right)\right)^k w_k\left(R,\theta,\phi,t - \frac{r-R}{c}\right). \tag{54}$$

When the solution consists of a finite number of spherical harmonics Y_{nm} up to order $n \leq P$, both the boundary condition (21) and the exterior evaluation formula (54) are exact. For smooth wave fields, the Fourier representation of u in the exterior converges uniformly, absolutely and exponentially fast. Hence we expect spectral accuracy with increasing P. Remarkably, the time retarded values of the auxiliary functions at (R,θ,ϕ) suffice to determine the solution everywhere in the exterior along the straight line with constant θ and ϕ.

3.3. Local NBC for multiple scattering

For simplicity, we first consider scattering from only two bounded disjoint scatterers, each surrounded by a sphere B_i of radius, $R_i, i = 1, 2$. Following the general formulation of Section 2.1, we let D_1 denote the unbounded region outside B_1 and D_2 denote the unbounded region outside B_2. Then the total scattered field u admits the unique decomposition $u = u_1 + u_2$ in

$D = D_1 \cap D_2$, where u_1 and u_2 are purely outgoing wave fields that satisfy (7)–(8) and (9)–(10), respectively.

Outside each sphere B_j, we now introduce local spherical coordinates (r_j, θ_j, ϕ_j), $j = 1, 2$. At B_1, for instance, the decomposition of u into an outgoing part u_1 and an incoming part u_2 then immediately yields the identity

$$\left(\frac{1}{c}\frac{\partial}{\partial t} + \frac{\partial}{\partial r_1} + \frac{1}{R_1}\right) u = \left(\frac{1}{c}\frac{\partial}{\partial t} + \frac{\partial}{\partial r_1} + \frac{1}{R_1}\right) u_1 + \left(\frac{1}{c}\frac{\partial}{\partial t} + \frac{\partial}{\partial r_1} + \frac{1}{R_1}\right) u_2. \tag{55}$$

To turn (55) into a practical boundary condition, we need to determine the outgoing and the incoming contributions on the right-hand side. For the outgoing part, we shall use (21) applied to u_1, whereas for the incoming contribution we shall use the explicit evaluation formula (54) applied to u_2. This immediately yields the exact NBC at B_1:

$$\left(\frac{1}{c}\frac{\partial}{\partial t} + \frac{\partial}{\partial r_1} + \frac{1}{R_1}\right) u = w_1^{(1)} + \left(\frac{1}{c}\frac{\partial}{\partial t} + \frac{\partial}{\partial r_1} + \frac{1}{R_1}\right) u_2, \tag{56}$$

where

$$\Big(\frac{1}{c}\frac{\partial}{\partial t} + \frac{k}{r_1}\Big) w_k^{(1)} = \frac{1}{4R_1^2}\Big(k(k-1) + \Delta_{S_1}\Big) w_{k-1}^{(1)} + w_{k+1}^{(1)} \tag{57}$$

for $k = 1, 2, \ldots$, and $w_0^{(1)} = 2u_1$. Here the functions $w_k^{(1)}$ correspond to the auxiliary functions associated with u_1 at B_1, whereas Δ_{S_1} denotes the Laplace-Beltrami operator (22) at B_1. Note that the functions $w_k^{(1)}$ are entirely determined by the values of u_1 (not u) at B_1 through their recursive definition (57), initialized by $w_0^{(1)} = 2u_1$.

In (56), the incoming part is determined through the evaluation formula (54) applied to u_2, that is

$$u_2(r_2, \theta_2, \phi_2, t) = \frac{R_2}{r_2} \sum_{k=0}^{P} \frac{2^{k-1}}{k!} \left(R_2\left(1 - \frac{R_2}{r_2}\right)\right)^k w_k^{(2)}\left(R_2, \theta_2, \phi_2, t - \frac{r_2 - R_2}{c}\right). \tag{58}$$

Here the auxiliary functions $w_k^{(2)}$, associated with u_2 at B_2, satisfy

$$\Big(\frac{1}{c}\frac{\partial}{\partial t} + \frac{k}{r_2}\Big) w_k^{(2)} = \frac{1}{4R_2^2}\Big(k(k-1) + \Delta_{S_2}\Big) w_{k-1}^{(2)} + w_{k+1}^{(2)} \tag{59}$$

for $k = 1, 2, \ldots$, and $w_0^{(2)} = 2u_2$.

The above derivation immediately generalizes to an arbitrary number of scatterers. Consider a situation with $J \geq 2$ scatterers and surround each scatterer by a sphere B_j of radius R_j, $j = 1, \ldots, J$. Again, we denote by $B = \bigcup_{j=1}^{J} B_j$ the entire artificial boundary and by D_j the unbounded region outside B_j. Hence the computational domain $\Omega = \bigcup_{j=1}^{J} \Omega_j$, where Ω_j denotes the finite computational region inside B_j. In the unbounded exterior region $D = \bigcap_{j=1}^{J} D_j$, we again split u into J purely outgoing waves, $u = u_1 + \cdots + u_J$, where each u_j solves a homogeneous wave equation similar to (7)–(8) in D_j.

When applied to J scatterers, the previous argument immediately yields at any B_j the exact local NBC:

$$\left(\frac{1}{c}\frac{\partial}{\partial t} + \frac{\partial}{\partial r_j} + \frac{1}{R_j}\right) u = w_1^{(j)} + \sum_{i \neq j} \left(\frac{1}{c}\frac{\partial}{\partial t} + \frac{\partial}{\partial r_j} + \frac{1}{R_j}\right) u_i, \tag{60}$$

where (r_j, θ_j, ϕ_j) denote local spherical coordinates at B_j. The auxiliary functions $w_k^{(j)}$, $k = 1, \ldots,$ are associated with u_j at B_j. They satisfy

$$\Big(\frac{1}{c}\frac{\partial}{\partial t} + \frac{k}{R_j}\Big) w_k^{(j)} = \frac{1}{4R_j^2}\Big(k(k-1) + \Delta_{S_j}\Big) w_{k-1}^{(j)} + w_{k+1}^{(j)} \tag{61}$$

with $w_0^{(j)} = 2u_j$. Now in (60), the incoming part is determined by adding the individual contributions from the other computational domains through the evaluation formula (54) applied to u_i at B_j:

$$u_i(r_i, \theta_i, \phi_i, t) = \frac{R_i}{r_i} \sum_{k=0}^{P} \frac{2^{k-1}}{k!} \left(R_i \left(1 - \frac{R_i}{r_i}\right)\right)^k w_k^{(i)} \left(R_i, \theta_i, \phi_i, t - \frac{r_i - R_i}{c}\right). \tag{62}$$

In fact the evaluation formula (54) is not only used in (60) but also needed to evaluate

$$w_0^{(j)} = 2u_j = 2\left(u - \sum_{i \neq j} u_i\right) \qquad \text{at } B_j. \tag{63}$$

The NBC (60)–(62) is completely local in the sense that it involves only derivatives and no integrals in space or time. Because the values of $w_k^{(i)}$ required in (62) are time-retarded, they are already known, so that the entire scheme remains explicit in time.

For solutions that consist of a superposition of spherical harmonics of order $n \leq P$, the boundary condition is exact. For smooth solutions the

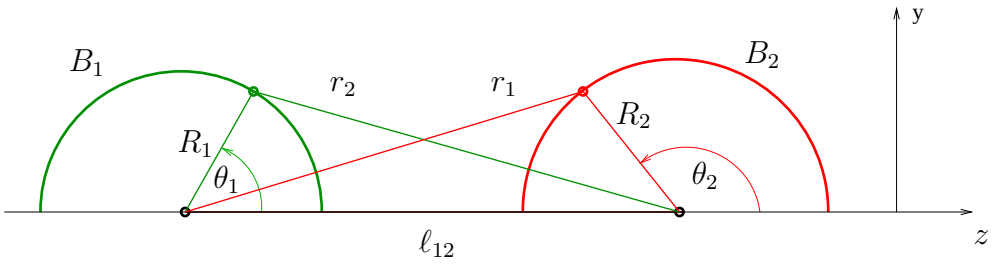

Figure 3: Local coordinates (r_1, θ_1) and (r_2, θ_2)

error due to truncation at P decreases exponentially fast with P. Hence it can be made arbitrarily small in a systematic fashion without moving the artifical boundaries any farther. In particular, the error due to truncation can easily be reduced below the discretization error due to the numerical scheme inside Ω. Hence the NBC is exact in the same sense as the boundary conditions in [17, 18, 25]. In practice we have found that small values of P often yield ample accuracy. Clearly the number of auxiliary functions used at different B_j do not need to be identical but can be judiciously chosen depending on the problem or the desired accuracy.

4. Implementation and finite difference discretization

First, we shall show how to efficiently evaluate the wave field u_i, outgoing from B_i, at any other artificial boundary component $B_j, j \neq i$, as in (60). Next, we shall present a typical finite difference discretization of the local NBC (60)–(62) and exhibit the full algorithm.

4.1. Exterior evaluation and local spline interpolation

Here for simplicity, we restrict the discussion to the situation with two scatterers only. In (56), the normal derivative of u_2 with respect to r_1 is obtained through a change of coordinates chosen such that the two z-axes and the two planes $\phi_1 = 0$ and $\phi_2 = 0$ coincide – see Fig. 3. Let ℓ_{12} denote the distance between the two origins. Then the coordinates of any point on

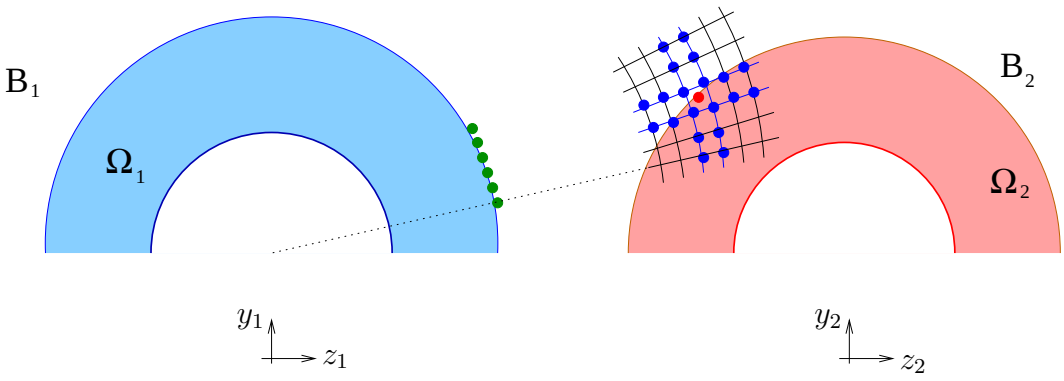

Figure 4: Evaluation of u_1 at B_2. Given the auxiliary functions, $w_k^{(1)}$, $k = 0, \ldots, P$ at B_1 defined in (57), we evaluate u_1 in the vicinity of B_2 at equispaced locations in (r_1, θ_1, ϕ_1) coordinates. From those values both u_1 and its partial derivatives with respect to t, r_1, θ_1 are approximated by finite differences and evaluated through local spline interpolation (69) at B_2.

B_1 in the (r_2, θ_2, ϕ_2)-coordinate system are given by

$$r_2 = \sqrt{R_1^2 - 2R_1\ \ell_{12}\ \cos\theta_1 + \ell_{12}^2}\ , \tag{64}$$

$$\theta_2 = \arcsin\left(R_1 \frac{\sin\theta_1}{r_2}\right), \qquad \theta_2 \in [-\pi/2, \pi/2], \tag{65}$$

$$\phi_2 = \phi_1. \tag{66}$$

Thus we can express the normal derivative at B_1 in terms of the radial and angular derivatives in (r_2, θ_2, ϕ_2)-coordinates as

$$\left.\frac{\partial}{\partial r_1}\right|_{r_1=R_1} = \alpha_{12}\big|_{r_1=R_1}(\theta_1)\frac{\partial}{\partial r_2} + \beta_{12}(\theta_1)\big|_{r_1=R_1}\frac{\partial}{\partial \theta_2}, \tag{67}$$

with

$$\alpha_{12}\big|_{r_1=R_1} = \frac{R_1 - \ell_{12}\cos\theta_1}{r_2}, \qquad \beta_{12}\big|_{r_1=R_1} = -\frac{\ell_{12}\sin\theta_1}{r_2^2}, \tag{68}$$

where r_2 and θ_2 are given by (64), (65).

Given the auxiliary functions, $w_k^{(1)}$, $k = 0, \ldots, P$ at B_1 defined in (57), we evaluate u_1 in the vicinity of B_2 at equispaced locations in (r_1, θ_1, ϕ_1) coordinates, as shown in Fig. 4. From those values both u_1 and its partial

derivatives with respect to t, r_1, θ_1 are computed by finite differences and then interpolated at B_2. To interpolate the values of u_1 or its partial derivatives at B_2, we use local spline interpolation, which we briefly recall in the one-dimensional case for the sake of completeness.

For given data points s_j at equispaced locations in one space dimension

$$s(x_j) = s_j, \qquad j = 0, \ldots, n-1,$$

the cubic spline interpolant in the sense of Akima [2] is defined as

$$s(x) = a_j + b_j(x - x_j) + c_j(x - x_j)^2 + d_j(x - x_j)^3, \qquad x_j \le x \le x_{j+1}. \quad (69)$$

Here the coefficients of the interpolating polynomial (69) are

$$\begin{aligned} a_j &= s_j(x_j), \\ b_j &= s'_j(x_j), \\ c_j &= \frac{1}{x_{j+1} - x_j} \left(3\frac{s_j(x_{j+1}) - s_j(x_j)}{x_{j+1} - x_j} - 2s'_j(x_j) - s'_j(x_{j+1}) \right), \\ d_j &= \frac{1}{(x_{j+1} - x_j)^2} \left(s'_j(x_j) + s'_j(x_{j+1}) - 2\frac{s'_j(x_{j+1}) - s'_j(x_j)}{x_{j+1} - x_j} \right), \end{aligned} \quad (70)$$

where the slopes $s'_j(x_j)$ are appropriately chosen finite difference approximations. The coefficients are calculated locally and do not require the solution of any large linear systems of equations – see [2] for further details.

4.2. Finite difference discretization

We shall now show how to discretize the local NBC for multiple scattering in (60)–(62) with a standard second order finite difference scheme. Again we consider J disjoint sub-domains Ω_j, $j = 1, \ldots, J$, and choose an equidistant grid in local spherical coordinates (r_j, θ_j, ϕ_j) along each artificial boundary, B_j, of radius R_j. We denote by N_j the corresponding radial index of those grid points located at $r_j = R_j$. Time is discretized at equidistant points $t_m = m\Delta t$, $m = 0, 1, \ldots$.

Next, we denote by U_{m,N_j} the values of the numerical solution at $r_j = R_j$ and time $t = t_m$. Moreover we denote by $W^{(j)}_{k,m}$ and $U^{(j)}_m$ the numerical approximations of $w^{(j)}_k$ and $u^{(j)}$ at $r_j = R_j - \Delta r/2$ and $t = t_m$, respectively. Note that both $W^{(j)}_{k,m}$ and $U^{(j)}_m$ are only stored along B_j, and not inside Ω_j.

The standard second order finite difference discretization of the wave equation cannot be used to advance U_{m,N_j} in time, as it involves the values U_{m,N_j+1}, which lie outside the computational domain Ω_j. Instead, we shall therefore apply the boundary condition (60) at $t = t_m + \Delta t/2$ and $r_j = R_j - (\Delta r/2)$, that is between the last two rows of grid points, U_{m,N_j-1} and U_{m,N_j}:

$$\begin{aligned}
&\frac{(U_{m+1,N_j} + U_{m+1,N_j-1}) - (U_{m,N_j} + U_{m,N_j-1})}{2c\Delta t} \\
&+\frac{(U_{m+1,N_j} + U_{m,N_j}) - (U_{m+1,N_j-1} + U^k_{m,N_j-1})}{2\Delta r} \\
&+\frac{U_{m+1,N_j} + U_{m+1,N_j-1} + U_{m,N_j} + U_{m,N_j-1}}{4R} = \frac{3}{2}W^{(j)}_{1,m} - \frac{1}{2}W^{(j)}_{1,m-1}.
\end{aligned} \tag{71}$$

Here, the value of $W^{(j)}_{1,m+1/2}$ at $t = t_m + \Delta t/2$ is extrapolated in time from $W^{(j)}_{1,m-1}$ and $W^{(j)}_{1,m}$, as in [25].

To advance the auxiliary functions $W^{(j)}_{k,m}$, we discretize (61) at $t = t_m + \Delta t/2$ and $r_j = R_j - (\Delta r/2)$, which yields

$$\begin{aligned}
&\frac{W^{(j)}_{k,m+1} - W^{(j)}_{k,m}}{\Delta t} + \frac{k}{2(R_j - \Delta r/2)}(W^{(j)}_{k,m+1} + W^{(j)}_{k,m}) \\
=&\frac{1}{8(R_j - \Delta r/2)^2}\left(\Delta^h_s + k(k-1)\right)(W^{(j)}_{k-1,m+1} + W^{(j)}_{k-1,m}) + \frac{3}{2}W^{(j)}_{k+1,m} - \frac{1}{2}W^{(j)}_{k+1,m-1},
\end{aligned}$$

with $W^{(j)}_{0,m+1} = 2U^{(j)}_{m+1}$.

In summary, the entire algorithm reads as follows:

Algorithm

- Initialize U_0 and U_1 in Ω.
- Set the auxiliary functions $W^{(j)}_{k,0}, W^{(j)}_{k,1}$ $k = 1, 2, \ldots, P$ and $U^{(j)}_0, U^{(j)}_1$, $j = 1, \ldots, J$ to zero.
- At each time step t_m and for every sub-domain Ω_j, $j = 1, \ldots, J$, given U_m, U_{m-1}, $U^{(j)}_m$, $U^{(j)}_{m-1}$, $W^{(j)}_{k,m}$, and $W^{(j)}_{k,m}$, $k = 0, 1, \ldots, P$:
  - advance $U_{m+1,\ell}$, $\ell \leq N_j - 1$ inside Ω_j;
  - advance U_{m+1,N_j} at B_j using (71);

– compute the outgoing part $U^{(j)}_{m+1}$ at $r_j = R_j - \Delta r/2$ from (62), (63) by using local spline interpolation, and set $W^{(j)}_{0,m+1} = 2U^{(j)}_{m+1}$;

– advance $W^{(j)}_{k,m+1}, k = 1, \ldots, P$, using (72).

The above algorithm is fully explicit and does not requires the solution of any large linear systems. Moreover, the interior and boundary unknowns in different subdomains Ω_j can be advanced in time independently of each other, except for the information transfer needed to compute $U^{(j)}_{m+1}$ through (63) in each time step. Remarkably, the information transfer of time retarded values between sub-domains occurs only across those parts of the artificial boundary, where outgoing rays intersect neighboring sub-domains, typically only across a fraction of the artificial boundary. Hence the information exchange between sub-domains is kept to a minimum. Further reduction of storage could probably be achieved by compression techniques [3, 29] applied to the past values of the auxiliary functions at B.

5. Numerical results

To assess the accuracy of the nonreflecting boundary condition for multiple scattering (60)–(62), we shall combine it with a finite difference method, as described in Section 4, and apply it to two test problems. First, we shall compute the radiating wave field of a transient off-centered point source in a homogeneous medium. Since the exact solution is known, we can study the accuracy both of the local NBC and the exterior evaluation formula, as the number of auxiliary functions P varies or the grid is refined. Second, we shall present computations for scattering of a plane wave from two sound-soft spheres. Both test problems are axisymmetric about the z-axis, so that the scattered field u is independent of ϕ.

5.1. Accuracy and convergence study

To verify the accuracy of the local NBC (21) and the exterior evaluation formula (54), we first consider an outgoing spherical wave propagating outward into a homogeneous medium with constant speed $c = 1$, which originates from a point source located at distance $d = 0.4$ from the origin. Its time dependence is determined by

$$g(t) = e^{-(t-\alpha)^2/\sigma^2}, \quad \alpha = 0.3, \quad \sigma = \frac{\alpha}{7 \log 10} \tag{72}$$

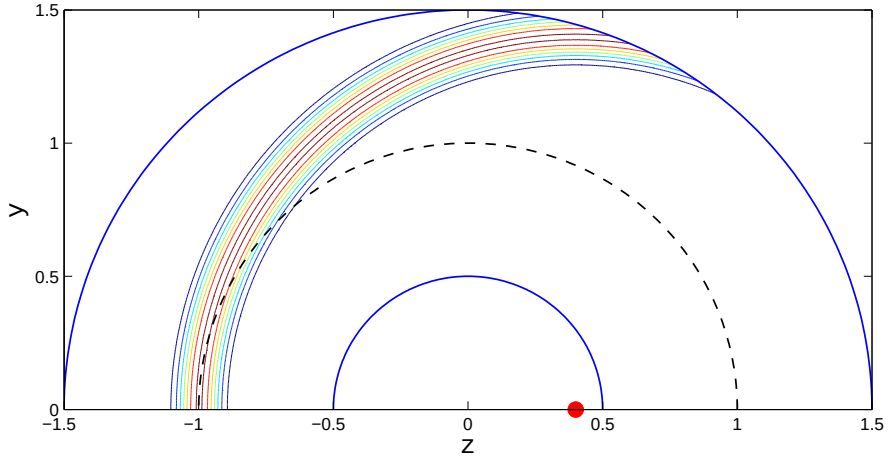

Figure 5: Contour lines of u obtained either from the numerical solution for $0.5 \leq r \leq 1$ or from the evaluation formula (54) for $1 < r \leq 1.5$. The point source is located at $x = 0$, $y = 0$, $z = 0.4$.

and vanishes outside the time window $[0, 0.6]$. This exact solution is used to initialize the numerical solution at $t = 0$ inside the computational domain $\Omega = \{(r, \theta) \,|\, 0.5 \leq r \leq 1, 0 \leq \theta \leq \pi\}$. At the artificial boundary B, located at $R = 1$, we impose (21) for varying P. Outside Ω, in the annular region $1 \leq r \leq 1.5$ directly adjacent to it, the solution is simply evaluated using (33) with $R = 1$. As shown in Fig. 5, the contour lines across B are smooth. In Fig. 6, we compare the numerical solution along the ray $\theta = \pi/2$ at time $t = 1$ for varying P with the exact solution. We observe how the solution significantly changes at low values of P, but rapidly converges with increasing P.

Next, the total L^2-error inside Ω vs. the mesh size h is shown in Fig. 7 for different values of P. For $P = 4$ we observe the expected global second-order convergence up to the finest mesh chosen here. We also observe the subtle interplay between the approximation error in the boundary condition, controlled by P, and that due to discretization in the interior of Ω. For small values of P, the error due to truncation tends to dominate, so that further mesh refinement does not improve the accuracy. In contrast, if we keep the mesh size h fixed, we observe no further improvement in the accuracy from increasing P. In general, convergence can only be achieved by systematically

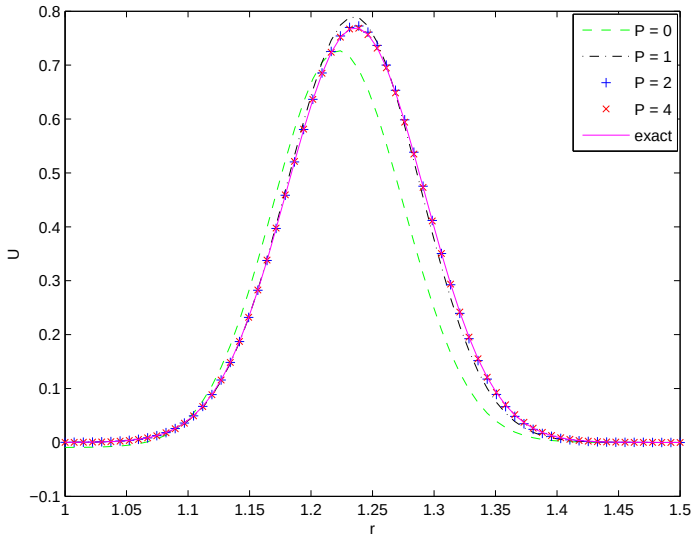

Figure 6: Evaluation of the scattered field u at $\theta = \frac{\pi}{2}$ and $t = 1$ for varying P.

reducing h while increasing P, simultaneously.

5.2. Plane wave scattering from two spheres

Next, we consider an incident plane wave packet,

$$u^{inc}(x, y, z, t) = e^{-125(z-0.3-t)^2},$$

impinging upon two sound-soft spheres centered about the z-axis and embedded in a homogenous medium with $c = 1$. Hence the scattered field u satisfies the time-dependent Dirichlet-type boundary condition, $u = -u^{inc}$, on the surface of the two obstacles. It is computed inside the two disjoint regions, Ω_1 and Ω_2, each surrounding an inner sound-soft spherical obstacle, by using the local NBC for multiple scattering (60)–(62). The left computational domain, Ω_1, corresponds to the region $0.5 < r_1 < 1$, in (r_1, θ_1, ϕ_1) local spherical coordinates centered about $x = 0, y = 0, z = -1$, and the right computational domain, Ω_2, corresponds to the region $0.5 < r_2 < 1$, in (r_2, θ_2, ϕ_2) local spherical coordinates centered about $x = 0, y = 0, z = 1.1$. Hence the distance between the two disjoint computational domains is 0.1 . Because the solution is axisymmetric, we can restrict the computations in

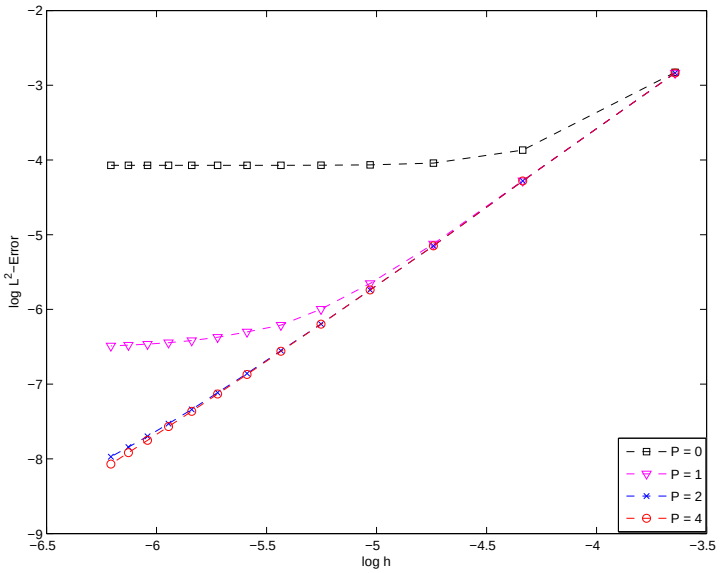

Figure 7: The total L^2-error is shown vs. the mesh size h for varying P.

each Ω_i to the two-dimensional region $0.5 < r_i < 1$, $0 \leq \theta_i \leq \pi$, $i = 1, 2$, where we use a 70×420 equidistant finite difference grid.

In Fig. 8, the total wave field $u+u^{inc}$ is shown at selected instants in time. At time $t = 0$, the right-moving incident plane wave has penetrated Ω_2. By the time $t = 0.5$, the incident plane wave has impinged upon the right sphere and generated a left-moving scattered wave. Then, the incident plane wave proceeds around the obstacle until it leaves Ω_2 at time $t \simeq 2$. Meanwhile the scattered wave has entered Ω_1 and impinged upon the left sphere at $t = 1.5$, creating yet another right-moving scattered wave. At $t = 2.3$ that secondary reflected wave has reached Ω_2 but still partly extends into Ω_1. The scattered waves bounce back and forth between the two obstacles while continuously radiating energy into the surrounding unbounded medium.

In Fig. 9 and Fig. 10, we illustrate the effect of truncating the NBC (60)–(62) at different values of P on the accuracy. To do so, we compare three numerical solutions, obtained with $P = 0$, $P = 1$ or $P = 4$ at two selected points inside the left computational domain Ω_1. At both locations we observe how small values of P, here $P = 0$ and $P = 1$, induce spurious

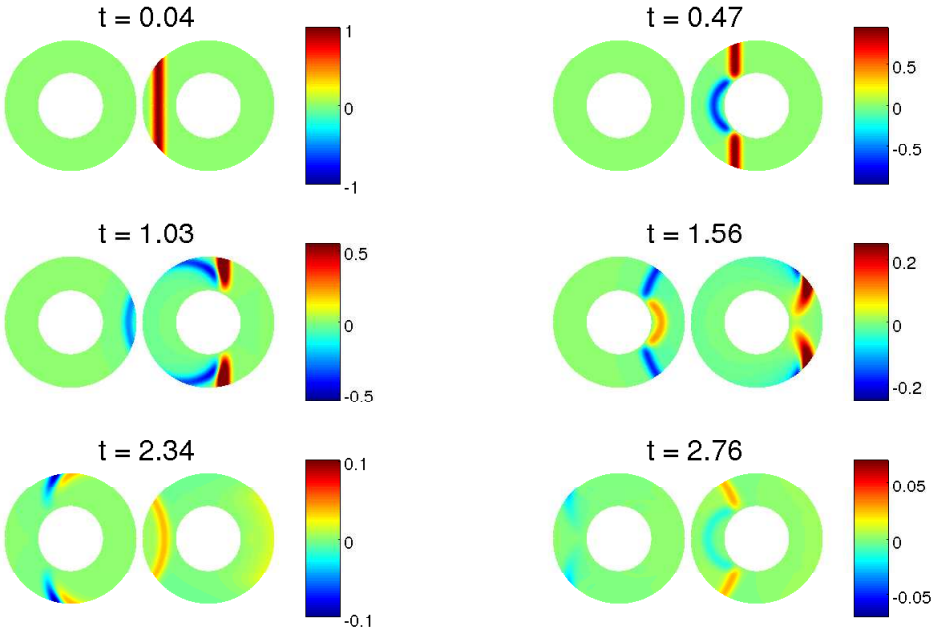

Figure 8: Plane wave scattering from two sound-soft spheres. The total wave field is shown at selected instants in time inside the computational domain, which consists of the two disjoint regions Ω_1 and Ω_2.

reflections at later times, which distort the total wave field once the initial plane wave packet has passed the observation site. Indeed setting $P = 0$ in the NBC corresponds to approximating the decomposition of u in the two purely outgoing wave fields u_1, u_2 outside Ω by two spherically symmetric wave fields, $u(x, y, z, t) \simeq u_1(r_1, t) + u_2(r_2, t)$. In that case the boundary condition for single scattering (21) reduces to the first order Bayliss-Turkel condition [6], whereas the exterior evaluation formula (54) simply propagates a spherically symmetric wave field into the unbounded exterior. Hence when $P = 0$, the effect of either obstacle onto the other is (crudely) replaced by that of a simple point source. At higher values of P, $P \geq 4$, the spurious reflections have vanished (at this scale).

Finally, to verify the overall stability of our numerical scheme, we show in Fig. 11 the long-time evolution of the L_2-norm of u in Ω for different values

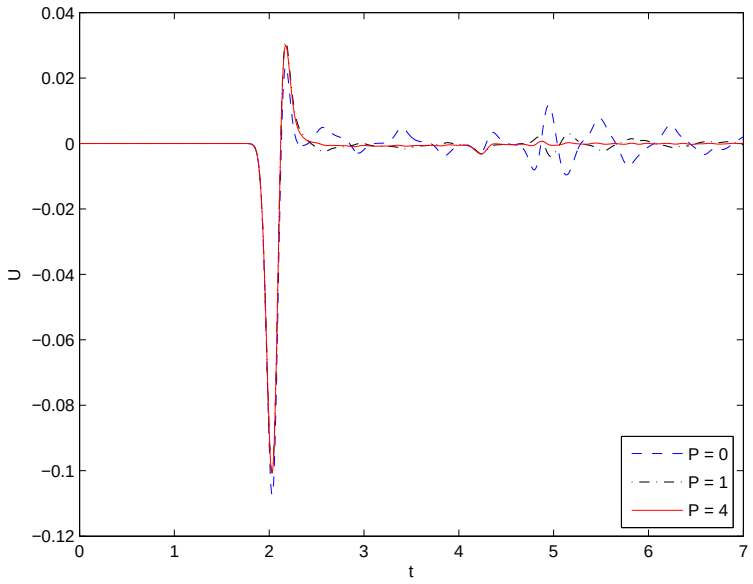

Figure 9: Plane wave scattering from two sound-soft spheres. The total wave field is shown vs. time at $x = 0, y = 0.75, z = -1$ inside the left computational domain Ω_1 for $P = 0, 1, 4$.

of P. For all values of P, we observe no growth or numerical instability even at very long times. At small values of P, spuriously reflected and propagated waves induce trapped wave energy inside Ω. At higher values of P, the energy more rapidly decays to vanishingly small values, as expected, while the wave energy is continuously radiated into the unbounded exterior.

6. Conclusion

We have derived a nonreflecting boundary condition (NBC) for time-dependent multiple scattering problems in three space dimensions, which holds when the artificial boundary B consists of a union of disjoint spheres B_j. It is given by (60)–(62) and avoids spurious reflection from B. The NBC is completely local both in space and time as it does not involve any integrals over B or the past of the solution. In fact, since the NBC involves only first-order normal and time derivatives, together with second-order tangential

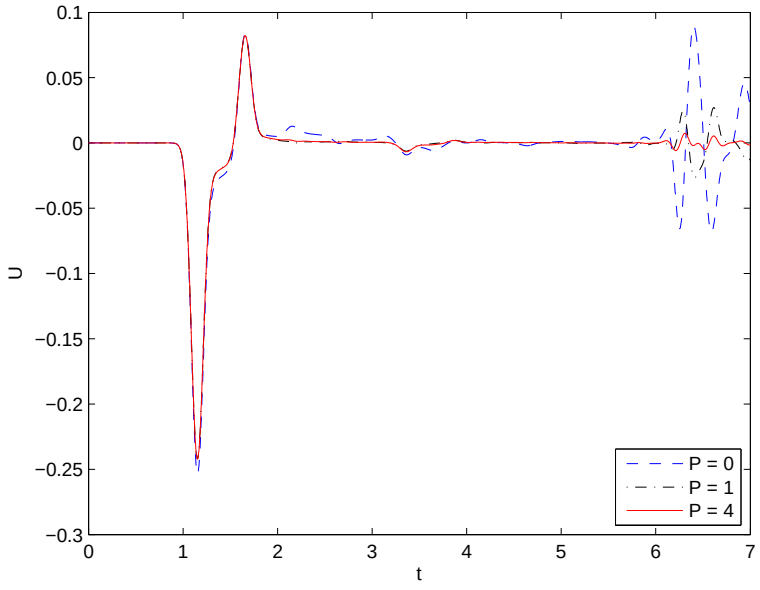

Figure 10: Plane wave scattering from two sound-soft spheres. The total wave field is shown vs. time at $x = 0, y = 0, z = -0.25$ inside the left computational domain Ω_1 for $P = 0, 1, 4$.

derivatives, at B, it is easily coupled with standard finite difference or finite element methods.

The derivation of our local NBC rests on the decomposition of the scattered field into purely outgoing wave fields, each evaluated at all other boundary components through the *exterior evaluation formula* (54). In fact, the exterior evaluation formula stands in its own right, even in situations of single scattering, as it permits to calculate the scattered field everywhere outside the computational domain. Remarkably, the information transfer of time retarded values between sub-domains occurs only across those parts of the artificial boundary, where outgoing rays intersect neighboring sub-domains, typically only across a fraction of the artificial boundary.

Since the artificial boundary no longer needs to be convex, the size of the computational domain can be chosen much smaller than with classical absorbing boundary conditions or perfectly matched layers (PML); moreover, the size of the computational domain no longer increases with the relative

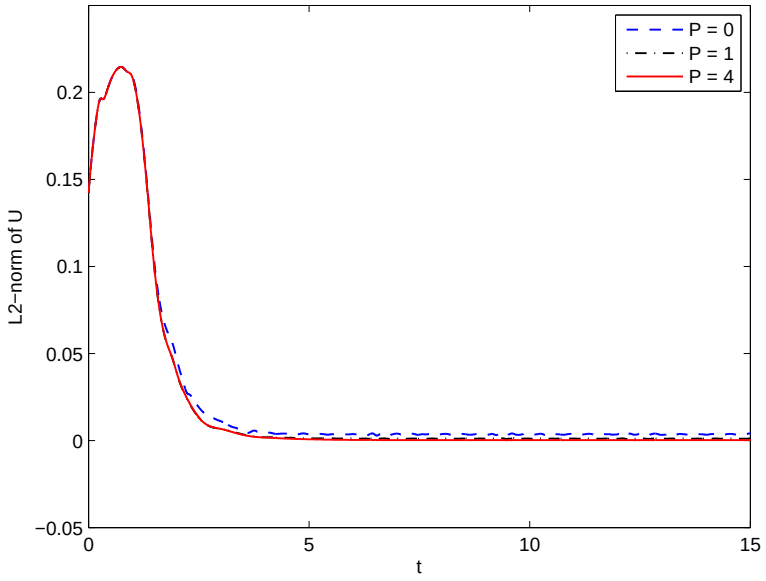

Figure 11: Plane wave scattering from two sound-soft spheres: the L_2-norm of the total wave field is shown vs. time for $P = 0, 1, 4$.

distance between the various sub-scatterers. Although the artificial boundary must be of simple geometric shape, here a union of disjoint spheres, the NBC is not tied to any particular coordinate system inside B_j, where the scatterer itself is arbitrary.

Because the NBC is local and yields spectral accuracy with an increasing number of auxiliary functions P, the computational work scales linearly with the number of unknowns at the artificial boundary. In practice, small values of P often yield ample accuracy. The storage required for the auxiliary functions is comparable to that required by any PML or NBC approach in situations of single scattering. Although the storage required for the auxiliary functions does increase linearly with the travel time between the sub-domains B_j, the computational effort is independent of the relative distances between scatterers. Hence, the full numerical scheme retains the global rate of convergence of the interior scheme, while the computational work and storage due to the NBC only involves a fraction of the computational effort inside B. Further reduction of storage could probably be achieved by compression

techniques [3, 29] applied to the past values of the auxiliary functions at B.

Appendix

In Lemma 1 and Lemma 2, we first derive two technical results. Then in Lemma 3, we prove that the solution of the linear system of equations (45) is explicitly given by (46).

Lemma 1.

$$\sum_{j=1}^{k} \frac{(-1)^{j+1}}{(k-j+1)!j!} = \begin{cases} \frac{2}{(k+1)!} & : \quad k = 2n-1,\ n = 1, 2, \cdots \\ 0 & : \quad k = 2n,\ n = 1, 2, \cdots . \end{cases} \tag{73}$$

Proof: *From the binomial theorem we immediately find*

$$\begin{aligned} 0 = (1-1)^{k+1} &= \sum_{j=0}^{k+1} (-1)^j \binom{k+1}{j} \\ &= \sum_{j=1}^{k} (-1)^j \binom{k+1}{j} + 1 + (-1)^{k+1}. \end{aligned}$$

Thus we have

$$-1 + (-1)^k = \sum_{j=1}^{k} (-1)^j \binom{k+1}{j} = \sum_{j=1}^{k} (-1)^j \frac{(k+1)!}{(k+1-j)!j!}.$$

Dividing each side by $-(k+1)!$*, we finally obtain*

$$\sum_{j=1}^{k} \frac{(-1)^{j+1}}{(k-j+1)!j!} = \frac{1 + (-1)^{k+1}}{(k+1)!},$$

which concludes the proof. □

Lemma 2. *For* $k \geq 0$ *we have*

$$\sum_{j=0}^{k} (-1)^j \binom{P-j}{k-j+1} \binom{P}{j} = (-1)^k \binom{P}{k+1}. \tag{74}$$

Proof:

We first prove the following formula:

$$\sum_{j=1}^{k}(-1)^{j+1}\binom{P-j}{k-j+1}\binom{P}{j} = \begin{cases} 2\binom{P}{k+1} & : \quad k=2n-1,\ n=1,2,\cdots \\ 0 & : \quad k=2n,\ n=1,2,\cdots . \end{cases} \tag{75}$$

Since

$$\begin{aligned}\sum_{j=1}^{k}(-1)^{j+1}\binom{P-j}{k-j+1}\binom{P}{j} &= \sum_{j=1}^{k}(-1)^{j+1}\frac{(P-j)!}{(k-j+1)!(P-k-1)!}\frac{P!}{(P-j)!j!} \\ &= \frac{P!}{(P-(k+1))!}\sum_{j=1}^{k}\frac{(-1)^{j+1})}{(k-j+1)!j!},\end{aligned}$$

we obtain by using Lemma 1 *that*

$$\sum_{j=1}^{k}(-1)^{j+1}\binom{P-j}{k-j+1}\binom{P}{j} = \frac{P!}{(P-(k+1))!}\begin{cases} \frac{2}{(k+1)!} & : \quad k=2n-1,\ n=1,2,\cdots \\ 0 & : \quad k=2n,\ n=1,2,\cdots \end{cases}$$

which corresponds to (75).

Next, we rewrite the left side of (74) as

$$\binom{P}{k+1} - \sum_{j=1}^{k}(-1)^{j+1}\binom{P-j}{k-j+1}\binom{P}{j} \tag{76}$$

and apply (75) to the second term in (76). The resulting expression equals the right side of (74), which concludes the proof of Lemma 2. □

Lemma 3. *The solution of the linear system of equations (45) is explicitly given by*

$$\tilde{\eta}_\ell = \sum_{j=0}^{\ell}(-1)^{\ell-j}\binom{P-j}{\ell-j}b_j. \tag{77}$$

Proof: *The proof is by induction on* ℓ.
For $\ell = 0$, *we obviously have* $\tilde{\eta}_0 = b_0$ *and hence (77) holds.*
For $\ell \geq 1$, *we now assume that (77) holds for* $k = 1, 2, \ldots, \ell-1$, *and rewrite it as*

$$\tilde{\eta}_\ell = b_\ell - \sum_{k=0}^{\ell-1}\binom{P-k}{\ell-k}\tilde{\eta}_k. \tag{78}$$

We now use (77) to replace $\tilde{\eta}_k$ in (78), which yields

$$\tilde{\eta}_\ell = b_\ell - \sum_{k=0}^{\ell-1} \sum_{j=0}^{k} \binom{P-k}{\ell-k} \binom{P-j}{k-j} (-1)^{k-j}\, b_j. \tag{79}$$

By reordering the terms in the double sum according to the identity,

$$\sum_{k=0}^{P-1} \sum_{j=0}^{k} a_{k,j} = \sum_{j=0}^{P-1} \sum_{k=j}^{P-1} a_{k,j}, \tag{80}$$

we then rewrite (79) as

$$\tilde{\eta}_\ell = b_\ell - \sum_{j=0}^{\ell-1} \sum_{i=j}^{\ell-1} \binom{P-i}{\ell-i} \binom{P-j}{i-j} (-1)^{i-j}\, b_j. \tag{81}$$

With $m = i - j$, this yields

$$\tilde{\eta}_\ell = b_\ell - \sum_{j=0}^{\ell-1} \sum_{m=0}^{\ell-j-1} \binom{P-j-m}{\ell-j-m} \binom{P-j}{m} (-1)^{m}\, b_j. \tag{82}$$

By applying Lemma 2 to the inner sum over m in (82), we find that (82) reduces to (77), which completes the proof. □

References

[1] S. Acosta and V. Villamizar: *Coupling of Dirichlet-to-Neumann boundary condition and finite difference methods in curvilinear coordinates for multiple scattering.* J. Comput. Phys. **229**, pp. 5498–5517, 2010

[2] H. Akima : *A new method of interpolation and smooth curve fitting based on local procedures.* J. of the ACM **17** (4), pp. 589–602, 1970

[3] B. Alpert, L. Greengard, and T. Hagstrom: *Rapid evaluation of nonreflecting boundary kernels for time-domain wave propagation.* SIAM J. Numer. Anal. **37** (4), pp. 1138–1164, 2000

[4] R. J. Astley: *Transient spheroidal elements for unbounded wave problems.* Comp. Meth. Appl. Mech. Engrng. **164**, pp. 3–15, 1998

[5] L. Banjai and S. Sauter: *Rapid solution of the wave equation in unbounded domains.* SIAM J. Num. Anal., pp. 227–249, 2008

[6] A. Bayliss and E. Turkel: *Radiation boundary conditions for wave-like equations.* Comm. Pure Appl. Math. **33**, pp. 707–725, 1980

[7] E. Bécache, S. Fauqueux, and P. Joly: *Stability of perfectly matched layers, group velocities and anisotropic waves.* J. Comput. Phys. **188** (2), pp. 399–433, 2003

[8] J.-P. Bérenger: *A perfectly matched layer for the absorption of electromagnetic waves.* J. Comput. Phys. **114** (2), pp. 185–200, 1994

[9] Q. Y. Chen, T. Tang, and Z.-H. Teng: *A fast numerical method for integral equations of the first kind with logarithmic kernel using mesh grading.* J. Comput. Math. **22** (2), pp. 287–298, 2004

[10] F. Collino and P. Monk: *The perfectly matched layer in curvilinear coordinates.* SIAM J. Sci. Comput. **19** (6), pp. 2061–2090, 1998

[11] B. Engquist and A. J. Majda: *Absorbing boundary conditions for the numerical simulation of waves.* Math. Comp. **31** (139), pp. 629–651, 1977

[12] A. A. Ergin, B. Shanker, and E. Michielssen: *Fast evaluation of three-dimensional transient wave fields using diagonal translation operators.* J. Comput. Phys. **146** (1), pp. 157–180, 1998

[13] D. Givoli: *Numerical Methods for Problems in Infinite Domains*, Elsevier, Amsterdam, 1992

[14] D. Givoli: *High-order local non-reflecting boundary conditions: a review.* Wave Motion **39**, pp. 319–326, 2004

[15] D. Givoli and B. Neta: *High-order nonreflecting boundary scheme for time-dependent waves.* J. Comp. Phys., **186**, pp. 24–46, 2003

[16] M. J. Grote: *Local nonreflecting boundary condition for Maxwell's equations.* Comput. Methods Appl. Mech. Engrg. **195**, pp. 3691–3708, 2006

[17] M. J. Grote and J. B. Keller: *Exact nonreflecting boundary conditions for the time dependent wave equation.* SIAM J. Appl. Math. **55** (2), pp. 280–297, 1995

[18] M. J. Grote and J. B. Keller: *Nonreflecting boundary conditions for time-dependent scattering.* J. Comput. Phys. **127** (1), pp. 52–65, 1996

[19] M. J. Grote and J. B. Keller: *On nonreflecting boundary conditions.* J. Comput. Phys. **122** (2), pp. 231–243, 1995

[20] M. J. Grote and C. Kirsch: *Dirichlet-to-Neumann boundary conditions for multiple scattering problems.* J. Comput. Phys. **201** (2), pp. 630–650, 2004

[21] M.J. Grote and C. Kirsch: *Nonreflecting boundary condition for time-dependent multiple scattering.* J. Comput. Phys. **221** (2), pp. 41–62, 2007

[22] M. J. Grote and I. Sim: *Perfectly matched layer for the second-order wave equation.* In Proc. of 9th Internat. Conf. on Math. and Numerical Aspects of Wave Propagation (WAVES 2009), pp. 370–371, held in Pau, France, June 15–19, 2009

[23] T. Ha-Duong, B. Ludwig, and I. Terrasse: *A Galerkin BEM for transient acoustic scattering by an absorbing obstacle.* Internat. J. Numer. Methods Engrg. **57** (13), pp. 1845–1882, 2003

[24] T. Hagstrom: *Radiation boundary conditions for the numerical simulation of waves.* Acta Numer. **8**, pp. 47–106, 1999

[25] T. Hagstrom and S.I. Hariharan: *A formulation of asymptotic and exact boundary conditions using local operators.* Appl. Numer. Math. **27** (4), pp. 403–416, 1998

[26] T. Hagstrom and T. Warburton: *A new auxiliary variable formulation of high-order local radiation boundary conditions: corner compatibility conditions and extensions to first-order systems.* Wave Motion **39** (4), pp. 327–338, 2004

[27] R. L. Higdon: *Numerical absorbing boundary conditions for the wave equation.* Math. Comp. **49**, pp. 65–90, 1987

[28] R. Huan and L. L. Thompson: *Accurate radiation boundary conditions for the time-dependent wave equation on unbounded domains.* Int. J. Numer. Meth. Engng. **47**, pp. 1569–1603, 2000

[29] C. Lubich and A. Schädle: *Fast convolution for nonreflecting boundary conditions.* SIAM J. Sci. Comput. **24** (1), pp. 161–182, 2002

[30] I. L. Sofronov: *Artificial boundary conditions of absolute transparency for two- and three-dimensional external time-dependent scattering problems.* European J. Appl. Math. **9** (6), pp. 561–588, 1998

[31] Z.-H. Teng: *Exact boundary condition for time-dependent wave equation based on boundary integral.* J. Comput. Phys. **190** (2), pp. 398–418, 2003

[32] L. Ting and M.J. Miksis: *Exact boundary conditions for scattering problems.* J. Acoust. Soc. Amer. **80** (6), pp. 1825–1827, 1986

[33] S. V. Tsynkov: *Numerical solution of problems on unbounded domains. A review.* Appl. Num. Math. **27**, pp. 465, 1998

[34] C. H. Wilcox: *A generalization of theorems of Rellich and Atkinson.* Proc. Amer. Math. Soc. **7**, pp. 271–276, 1956

LATEST PREPRINTS

No.	Author: *Title*
2010-04	**Marcus Grote, Imbo Sim** *Local Nonreflecting Boundary Condition for Time-Dependent Multiple Scattering*
2010-03	**Marcus Grote, Viviana Palumberi, Barbara Wagner, Andrea Barbero, Ivan Martin** *Dynamic Formation of Oriented Patches in Chondrocyte Cell Cultures*
2010-02	**David Cohen, Ernst Hairer** *Linear Energy-Preserving Integrators for Poisson Systems*
2010-01	**Assyr Abdulle, Marcus J. Grote** *Finite Element Heterogeneous Multiscale Method for the Wave Equation*
2009-06	**Marcus J. Grote, Imbo Sim** *Efficient PML for the Wave Equation*
2009-05	**Francesco Amoroso, Evelina Viada** *Small Points on Subvarieties of a Torus*
2009-04	**Evelina Viada** *A Functorial Lower Bound for the Essential Minimum of Varieties in a Power of an Elliptic Curve*
2009-03	**Francesco Amoroso, Evelina Viada** *Small Points on Rational Subvarieties of Tori*
2009-02	**Marcus J. Grote, Teodora Mitkova** *Explicit Local Time-Stepping Methods for Maxwell's Equations*
2009-01	**Marcus J. Grote, Imbo Sim** *On Local Nonreflecting Boundary Conditions for Time Dependent Wave Propagation*
2008-05	**David Cohen, Xavier Raynaud** *Geometric Finite Difference Schemes for the Generalised Hyperelastic-Rod Wave Equation*
2008-04	**Marcus J. Grote, Dominik Schötzau** *Convergence Analysis of a Fully Discrete DG Method for the Wave Equation*